

SEARCH FOR PHOTINOS IN  $e^+e^-$  ANNIHILATION\*

John Ellis<sup>§</sup> and J. S. Hagelin  
Theory Group, Stanford Linear Accelerator Center  
Stanford University, Stanford, CA 94305

ABSTRACT

We discuss the pair production of massive photinos or other neutral gauginos in  $e^+e^-$  annihilation. We present cross sections for  $e^+e^- \rightarrow \tilde{\gamma}\tilde{\gamma}$  and  $e^+e^- \rightarrow \tilde{\gamma}\tilde{\gamma}\gamma$  including finite mass effects for both the selectron and the gaugino. Experimental signatures are a possible pair of photons from  $\tilde{\gamma}$  decay each with  $\langle E_\gamma \rangle = 1/4 E_{\text{c.m.}}$  and a single soft photon in the case of radiative pair production. We exhibit the domains of selectron and gaugino masses and of the supersymmetry breaking scale parameter that could be probed by dedicated searches, pointing out that the present PETRA and PEP centre-of-mass energies are nearly ideal for light gaugino hunts.

Submitted to Physics Letters B

---

\* Work supported by the Department of Energy, contract DE-AC03-76SF00515.

<sup>§</sup> On leave of absence from Theory Division, CERN, CH1211-Geneva, Switzerland.

There is presently great interest in theories with broken supersymmetry,<sup>1</sup> much of it stimulated by the hope such theories offer<sup>2</sup> for alleviating the hierarchy problem associated with the weak interaction scale. So far there is considerable phenomenological frustration, since no experimental signature of supersymmetry has yet been detected.<sup>3</sup> Supersymmetric partners of all the known light particles should exist with masses less than about 1 TeV if the desired technical improvement in the hierarchy problem is indeed to be obtained. However, within this range there is considerable flexibility in the possible spectrum of supersymmetric partner particles. Spin-zero partners of right- and left-handed leptons, such as the selectrons  $\tilde{e}_{L,R}$  may<sup>3</sup> or may not<sup>4,5</sup> have the same mass, and may<sup>3</sup> or may not<sup>4,5</sup> have masses  $\lesssim m_W/2$ . The neutral and colourless gaugino mass eigenstates may<sup>3</sup> or may not<sup>4,5</sup> be unmixed superpartners of the gauge boson eigenstates  $\gamma$  and  $Z^0$ . The gluino, and the photino if it is a mass eigenstate, may<sup>3</sup> or may not<sup>4,5</sup> have a very small mass. The lightest supersymmetric fermion may be the photino  $\tilde{\gamma}$  or gravitino<sup>3</sup>  $\tilde{G}$ , or perhaps a neutral shiggs fermion<sup>4</sup>  $\tilde{H}$ . Phenomenological calculations and experimental searches should be rather broad-band until we have a better idea under which lamppost to look. To date most calculations<sup>3,6</sup> of processes involving colourless neutral gauginos have focussed on the possibility of an (almost) massless photino. Estimates have been made<sup>6</sup> of the cross sections for  $e^+e^- \rightarrow \tilde{\gamma}\tilde{\gamma}$  in the limit of negligible  $\tilde{\gamma}$  mass and for  $e^+e^- \rightarrow \tilde{\gamma}\tilde{\gamma}\gamma$  in the limit of negligible photino mass and large selectron mass. We understand<sup>7</sup> that an experimental search is under way for  $e^+e^- \rightarrow \tilde{\gamma}\tilde{\gamma}$  followed by two  $\tilde{\gamma} \rightarrow \gamma + \tilde{G}$  decays.

In this paper we calculate exactly the tree-level cross sections for  $e^+e^- \rightarrow \tilde{\gamma}\tilde{\gamma}$ , or any other pair of neutral gauginos, for all values of the

photino and selectron masses. We then discuss the values of  $m_{\tilde{\gamma}}$ ,  $m_{\tilde{e}}$  and the supersymmetry breaking scale<sup>3</sup>  $\sqrt{d}$  for which one would hope to observe  $e^+e^- \rightarrow \tilde{\gamma}\tilde{\gamma}$  followed by two  $\tilde{\gamma} \rightarrow \gamma + \tilde{G}$  decays. We then calculate exactly the cross section for  $e^+e^- \rightarrow \tilde{\gamma}\tilde{\gamma}\tilde{\gamma}$  for arbitrary  $m_{\tilde{\gamma}}$  but for  $m_{\tilde{e}} \gg E_{c.m.}$ , and show how one can get an approximation to the cross section for arbitrary  $m_{\tilde{\gamma}}$  and  $m_{\tilde{e}}$  which is valid in the limit of a soft bremsstrahlung  $\gamma$  which accounts for most of the radiative cross section. We then discuss the ranges of  $m_{\tilde{\gamma}}$  and  $m_{\tilde{e}}$  which can be explored in a dedicated search for  $e^+e^- \rightarrow \gamma +$  unobserved neutrals. We find that this indirect method gives access to higher selectron masses than can be observed directly.<sup>8,9</sup> Our calculations can be carried over to other neutral gauginos. We stress that one does not gain substantially in sensitivity to the selectron mass by doing experiments at centre-of-mass energies higher than those currently attainable at PEP and PETRA.

We will be considering the production of massive gaugino pairs through selectron  $\tilde{e}$  exchange. There are two selectrons  $\tilde{e}_{L,R}$  which are supersymmetric partners of the left- and right-handed electron, respectively.<sup>1</sup> There is no mixing<sup>4,5,10</sup> between selectrons, smuons  $\tilde{\mu}$  and staus  $\tilde{\tau}$  in the classes of spontaneously broken supersymmetric theories that we prefer. Moreover, we expect off-diagonal mass matrix elements between the  $\tilde{e}_L$  and  $\tilde{e}_R$  to be suppressed by  $O(m_e/m_{\tilde{e}})$  and hence negligible.<sup>5</sup> On the other hand, in general we do not expect the  $\tilde{e}_L$  and  $\tilde{e}_R$  masses to be identical. In many spontaneously broken supersymmetric theories<sup>4,5</sup> the  $\tilde{e}_L$  is heavier than the  $\tilde{e}_R$  because the left-handed SU(2) weak interactions give a large extra contribution to  $m_{\tilde{e}_L}$ . Therefore we will separate the cross sections due to  $\tilde{e}_L$  and  $\tilde{e}_R$  exchange: if they are degenerate our cross sections should be increased by a

factor of two. Separating the  $\tilde{e}_L$  and  $\tilde{e}_R$  exchanges is also convenient when one considers the production of massive neutral gauginos other than the photino. The couplings of the photino to  $e_L \tilde{e}_L$  and  $e_R \tilde{e}_R$  are identical:<sup>1</sup>

$$\mathcal{L} = e\sqrt{2} \left[ \tilde{e}_L^- \bar{e}_L \left( \frac{1+\gamma_5}{2} \right) \tilde{\gamma} + \tilde{e}_R^- \bar{e}_R \left( \frac{1-\gamma_5}{2} \right) \tilde{\gamma} \right] + \text{h.c.} \quad , \quad (1)$$

but those of pure SU(2) or U(1)<sub>Y</sub> gauginos are not. For example the U(1)<sub>Y</sub> gaugino (the Bino  $\tilde{B}$ ) has couplings

$$\mathcal{L} = -\frac{e\sqrt{2}}{\cos\theta_W} \left[ \frac{1}{2} \tilde{e}_L^- \bar{e}_L \left( \frac{1+\gamma_5}{2} \right) \tilde{B} + \tilde{e}_R^- \bar{e}_R \left( \frac{1-\gamma_5}{2} \right) \tilde{B} \right] + \text{h.c.} \quad . \quad (2)$$

It will be easy to use eq. (2) to make the appropriate substitutions in our cross sections for  $\tilde{\gamma}$  production derived using eq. (1). Since  $\cos\theta_W \simeq 0.89$  is close to unity, the limits on  $\tilde{B}$  will be almost indistinguishable from our prospective  $\tilde{\gamma}$  limits if  $m_{\tilde{e}_R} \ll m_{\tilde{e}_L}$ , but would be somewhat weaker if  $m_{\tilde{e}_L} \ll m_{\tilde{e}_R}$ , a case which seems to us unlikely.<sup>5</sup> It is useful to recall<sup>3</sup> that in the local limit of  $m_{\tilde{e}} \gg$  typical momentum transfer,  $\tilde{e}_R$  exchange gives an effective four-fermion interaction

$$\mathcal{L}_{\text{eff}} = \frac{2e^2}{m_{\tilde{e}_R}^2} \tilde{\gamma}^- \left( \frac{1+\gamma_5}{2} \right) e^- \bar{e}^- \left( \frac{1-\gamma_5}{2} \right) \tilde{\gamma} \quad (3)$$

which can be Fierz-transformed to become

$$\mathcal{L}_{\text{eff}} = \frac{e^2}{m_{\tilde{e}_R}^2} \tilde{\gamma}^- \gamma^\mu \left( \frac{1-\gamma_5}{2} \right) \tilde{\gamma} \bar{e}^- \gamma_\mu \left( \frac{1+\gamma_5}{2} \right) e^- \quad . \quad (4)$$

Note that, because of Fermi statistics, identical massive neutral gauginos with total angular momentum one can only be produced in a relative P-wave and hence only the  $(\bar{\tilde{\gamma}} \gamma^\mu \gamma_5 \tilde{\gamma})$  part of eq. (4) actually contributes to physical cross sections. Therefore if one adds to eq. (4) the corresponding interaction due to  $\tilde{e}_L$  exchange one gets an axial-axial interaction if

$$m_{\tilde{e}_L} = m_{\tilde{e}_R} \text{ and parity is conserved as expected in this case.}$$

After these preliminaries we are now in a position to quote the result of the trivial calculation of  $e^+e^- \rightarrow \tilde{\gamma}\tilde{\gamma}$  for massive photinos and arbitrary

$$m_{\tilde{e}_R} :$$

$$\begin{aligned} \frac{d\sigma(e^+e^- \rightarrow \tilde{\gamma}\tilde{\gamma})}{d(\cos\theta_{\tilde{\gamma}})} &= \frac{\pi\alpha^2 s\beta^3}{4} \\ &\times \frac{(\Delta M^2 + \frac{s}{2})^2 (1 + \cos^2\theta_{\tilde{\gamma}}) - s \left[ 2(\Delta M^2 + \frac{s}{2}) - \frac{m_{\tilde{\gamma}}^2 - s}{4} \right] \cos^2\theta_{\tilde{\gamma}} + \frac{s^2\beta^2}{4} \cos^4\theta_{\tilde{\gamma}}}{\left[ (\Delta M^2 + \frac{s}{2})^2 - \frac{s^2\beta^2}{4} \cos^2\theta_{\tilde{\gamma}} \right]^2} \end{aligned} \quad (5)$$

where  $s \equiv E_{\text{c.m.}}^2$ ,  $\Delta M^2 \equiv m_{\tilde{e}_R}^2 - m_{\tilde{\gamma}}^2$  and  $\beta \equiv (1 - 4m_{\tilde{\gamma}}^2/s)^{1/2}$ . Note that there is no forward-backward asymmetry when we sum over  $\tilde{\gamma}$  polarizations. When integrated over  $\cos\theta_{\tilde{\gamma}}$ , eq. (5) yields

$$\begin{aligned} \sigma(e^+e^- \rightarrow \tilde{\gamma}\tilde{\gamma}) &= \frac{2\pi\alpha^2\beta}{s} \left( \Delta M^4 + \frac{s}{2} m_{\tilde{e}_R}^2 \right) \\ &\times \left[ \frac{1}{\Delta M^4 + s m_{\tilde{e}_R}^2} - \frac{1}{s\beta(\Delta M^2 + \frac{s}{2})} \ln \left( \frac{\Delta M^2 + \frac{s}{2} (1+\beta)}{\Delta M^2 + \frac{s}{2} (1-\beta)} \right) \right] . \end{aligned} \quad (6)$$

It is instructive to consider various limiting cases of the cross sections [eqs. (5), (6)]. In the limit  $m_{\tilde{\gamma}} \rightarrow 0$  the differential cross section reduces

to the result in footnote 4 of ref. 6 (once the latter is summed over  $\tilde{\gamma}$  polarizations), while the total cross section [eq. (6)] becomes

$$\sigma(e^+e^- \rightarrow \tilde{\gamma}\tilde{\gamma}) = \frac{\pi\alpha^2}{s} \left[ 1 + \frac{m_{\tilde{e}_R}^2}{m_{\tilde{e}_R}^2 + s} - \frac{2m_{\tilde{e}_R}^2}{s} \ln\left(\frac{m_{\tilde{e}_R}^2 + s}{m_{\tilde{e}_R}^2}\right) \right] . \quad (7)$$

In the local limit  $s/m_{\tilde{e}_R}^2 \ll 1$  the differential cross section [eq. (5)] becomes

$$\frac{d\sigma(e^+e^- \rightarrow \tilde{\gamma}\tilde{\gamma})}{d(\cos\theta_{\tilde{\gamma}})} = \frac{\pi\alpha^2 s \beta^3}{4m_{\tilde{e}_R}^4} \left( 1 + \cos^2\theta_{\tilde{\gamma}} \right) \quad (8)$$

while the total cross section [eq. (6)] becomes

$$\sigma(e^+e^- \rightarrow \tilde{\gamma}\tilde{\gamma}) = \frac{\pi\alpha^2 s \beta^3}{3m_{\tilde{e}_R}^4} . \quad (9)$$

Note the characteristic P-wave phase space factor  $\beta^3 = (1 - 4m_{\tilde{\gamma}}^2/s)^{3/2}$  appearing in eq. (9). It is noteworthy that the detailed finite mass total cross section [eq. (6)] is actually rather well approximated (to  $\pm 5\%$  in the kinematic regions of interest) by the  $m_{\tilde{\gamma}} = 0$  cross section [eq. (7)] multiplied by the P-wave phase space factor  $\beta^3$  which is compulsory only in the local limit [eq. (9)]. This completes our discussion of the cross section for  $e^+e^- \rightarrow \tilde{\gamma}\tilde{\gamma}$  and now we turn to experimental signatures.

If the gravitino  $\tilde{G}$  is lighter than the photino, the dominant decay mode of the  $\tilde{\gamma}$  is expected<sup>3</sup> to be  $\tilde{\gamma} \rightarrow \gamma + \tilde{G}$  with a decay width<sup>3,9,11</sup>

$$\Gamma(\tilde{\gamma} \rightarrow \gamma + \tilde{G}) = \frac{m_{\tilde{\gamma}}^5}{8\pi d^2} \quad (10)$$

where the parameter  $d$  has the dimension of  $(\text{mass})^2$  and measures<sup>3</sup> the scale of supersymmetry breaking. In many models  $\sqrt{d} = O(1)$  TeV. The signatures for  $e^+e^- \rightarrow \tilde{\gamma}\tilde{\gamma}$  are therefore production of a pair of photons, each having an average of one-half of the beam energy, not back-to-back unless the photino mass is much smaller than  $1/2 E_{\text{c.m.}}$ , with a reasonably isotropic angular distribution tending to  $1 + \cos^2\theta$  when  $m_{\tilde{\gamma}} \ll E_{\text{c.m.}} \ll m_{\tilde{e}}$ , and perhaps produced an observable distance from the interaction point as indicated in fig. 1.

For example, if  $\sqrt{d} = 1$  TeV a photino with mass 1 GeV would live about  $2 \times 10^{-11}$  seconds, and thus would travel several centimeters before decaying if it were produced at a beam energy of 15 GeV. Figure 2 shows the domain of the  $(m_{\tilde{\gamma}}, \sqrt{d})$  plane that could be explored at  $E_{\text{c.m.}} = 30$  GeV given a sensitivity to such  $e^+e^- \rightarrow \tilde{\gamma}\tilde{\gamma} + \text{unobserved neutrals}$  events of  $10^{-38} \text{ cm}^2$  corresponding to an integrated luminosity of  $10^2 \text{ pb}^{-1}$ . Below the diagonal line both photinos decay within one meter of the interaction point. If  $\sqrt{d}$  lies above this diagonal line, the photinos do not decay inside the apparatus and one has no experimental signature for  $e^+e^- \rightarrow \tilde{\gamma}\tilde{\gamma}$ . As indicated in fig. 2, the position of the diagonal line varies slightly with the selectron mass upon which the production cross section depends [eq. (6)]. We exhibit the constraint on  $m_{\tilde{\gamma}}$  and  $\sqrt{d}$  which is valid for  $m_{\tilde{e}} \lesssim 200$  GeV,  $m_{\tilde{e}} \lesssim 100$  GeV, and  $m_{\tilde{e}} \sim 15$  GeV (near the present experimental bound). For  $m_{\tilde{e}} \gtrsim 200$  GeV the cross section for  $e^+e^- \rightarrow \tilde{\gamma}\tilde{\gamma}$  drops below  $10^{-38} \text{ cm}^2$  at  $E_{\text{c.m.}} = 30$  GeV and the constraint disappears. Also, the P-wave phase space factor pushes the cross section below  $10^{-38} \text{ cm}^2$  at  $E_{\text{c.m.}} = 30$  GeV when one ventures beyond the solid vertical line in fig. 2; we will return to interpret the dashed vertical line later. Finally we observe that the domain of  $(m_{\tilde{\gamma}}, \sqrt{d})$

accessible to  $e^+e^- \rightarrow \tilde{\gamma}\tilde{\gamma}$  experiments is different from that accessible to an electron beam dump experiment,<sup>11</sup> which is also depicted roughly in fig. 2.

One can also look for the radiative process  $e^+e^- \rightarrow \tilde{\gamma}\tilde{\gamma}\gamma$  via the spectator bremsstrahlung  $\gamma$ . This process is very analogous to the reaction  $e^+e^- \rightarrow \nu\bar{\nu}\gamma$  which has been proposed<sup>12,13</sup> as a way of counting the number of neutrino species  $N_\nu$ , which for us is just an annoying background. The cross section for  $e^+e^- \rightarrow \nu\bar{\nu}\gamma$  at  $E_{\text{c.m.}} \ll m_{Z^0}$  has been computed<sup>12</sup> for massless neutrinos:

$$\frac{d^2\sigma}{dx_\gamma d(\cos\theta_\gamma)} = \frac{G_F^2 \alpha}{6\pi^2} \left[ N_\nu (g_V^2 + g_A^2) + 2(g_V + g_A + 1) \right] \frac{s}{x_\gamma (\sin^2\theta_\gamma)} \times \left[ (1-x_\gamma) \left(1 - \frac{x_\gamma}{2}\right)^2 + \frac{x_\gamma^2}{4} (1-x_\gamma) \cos^2\theta_\gamma \right] \quad (11)$$

where  $x_\gamma \equiv 2E_\gamma/E_{\text{c.m.}}$ . It is obvious from the form of  $\mathcal{L}_{\text{eff}}$  [eq. (4)] that in the local limit the differential cross section for  $e^+e^- \rightarrow \tilde{\gamma}\tilde{\gamma}$  has exactly the same shape as eq. (11) (see fig. 3) but has a different prefactor:

$$\frac{G_F^2 \alpha}{6\pi^2} \left[ N_\nu (g_V^2 + g_A^2) + 2(g_V + g_A + 1) \right] \rightarrow \frac{2}{3} \frac{\alpha^3}{m_{\tilde{e}_R}} \quad (12)$$

in the limit  $m_{\tilde{\gamma}} \ll E_{\text{c.m.}} \ll m_{\tilde{e}_R}$ . We have not calculated  $d^2\sigma/dx_\gamma d(\cos\theta_\gamma)$  for the most general values of  $m_{\tilde{\gamma}}$  and  $m_{\tilde{e}}$  (cries of shame!), but believe for the following reasons that we can estimate it reliably. In the local limit  $E_{\text{c.m.}} \ll m_{\tilde{e}}$ , the only effect of finite  $m_{\tilde{\gamma}}$  is to multiply the cross section [eqs. (11), (12)] by a P-wave phase space factor  $[1 - 4m_{\tilde{\gamma}}^2/s(1-x_\gamma)]^{3/2}$  for all values of  $x_\gamma$  and  $\cos\theta_\gamma$ . In point of fact, as seen in fig. 3, the cross section [eq. (11)] is sharply peaked towards small  $x_\gamma$ , corresponding to soft bremsstrahlung. General theorems<sup>14</sup> tell us that in the limit as  $x_\gamma \rightarrow 0$  any radiative cross section for  $e^+e^- \rightarrow X\gamma$  looks like



$$\frac{d^2\sigma}{dx_\gamma d(\cos\theta_\gamma)} \approx \frac{2\alpha}{\pi} \frac{1}{x_\gamma} \frac{1}{\sin^2\theta_\gamma} \sigma(e^+e^- \rightarrow X) \quad (13)$$

It is therefore a reasonable approximation to use Eq. (13) together with the general cross section [eq. (6)] obtained for  $e^+e^- \rightarrow \tilde{\gamma}\tilde{\gamma}$ . Furthermore one can separate the P-wave phase space factor  $\beta^3 = (1 - 4m_{\tilde{\gamma}}^2/s)^{3/2}$  from the general cross section for  $e^+e^- \rightarrow \tilde{\gamma}\tilde{\gamma}$  (which we have seen factorizes approximately into a phase space factor multiplying the cross section valid for a finite  $m_{\tilde{e}}$  with  $m_{\tilde{\gamma}} = 0$ ) and replace  $s$  in  $\beta^3$  with  $s(1-x_\gamma)$  in order to keep the correct P-wave phase space factor (above). This Ansatz provides a conservative account of the  $\tilde{e}$  propagator effects in  $e^+e^- \rightarrow \tilde{\gamma}\tilde{\gamma}\gamma$  which in fact will be less severe than for  $e^+e^- \rightarrow \tilde{\gamma}\tilde{\gamma}$  due to the finite energy carried off by the photon. We have used this Ansatz to draw fig. 4 and the dashed vertical line in fig. 2.

We see from fig. 3 that there is a premium on detecting the bremsstrahlung photon down to small  $x_\gamma$  and  $\theta_\gamma$ . After consulting our experimental colleagues we have calculated cross sections for  $x_\gamma \gtrsim 0.2$  (corresponding to 3 GeV at  $E_{\text{c.m.}} = 30$  GeV) and  $|\cos\theta_\gamma| \lesssim 0.94$  (corresponding to  $20^\circ < \theta_\gamma < 160^\circ$ ). Figure 4 shows the domain of  $m_{\tilde{e}}$  and  $m_{\tilde{\gamma}}$  for which the cross section for  $e^+e^- \rightarrow \tilde{\gamma}\tilde{\gamma}\gamma$  at  $E_{\text{c.m.}} = 30$  GeV subject to these cuts is  $\gtrsim 10^{-38} \text{ cm}^2$ , also suggested by our experimental colleagues. [Since the cross section is  $\propto m_{\tilde{e}}^{-4}$  for large  $m_{\tilde{e}}$ , even a sensitivity to cross sections of  $10^{-37} \text{ cm}^2$  would be sufficient to probe  $m_{\tilde{e}} \lesssim 40$  GeV.] For comparison, fig. 4 also shows the domains of  $m_{\tilde{e}}$  and  $m_{\tilde{\gamma}}$  accessible to other experimental searches. There is a lower limit on  $m_{\tilde{e}}$  from  $e^+e^- \rightarrow \tilde{e}^+\tilde{e}^-$  searches of about<sup>8</sup> 17 GeV which is

essentially independent of  $m_{\tilde{\gamma}}$ . There is also a potential<sup>9</sup> limit coming from  $e^+e^- \rightarrow e\tilde{e}\tilde{\gamma}$  which has a kinematic limit at  $m_{\tilde{e}} + m_{\tilde{\gamma}} \lesssim E_{\text{c.m.}}$ . An upper limit of  $10^{-38} \text{ cm}^2$  on this cross section<sup>15</sup> would probe quite close to this limit, as seen from the dashed line in fig. 4, which corresponds to  $m_{\tilde{e}} + m_{\tilde{\gamma}} \lesssim 27 \text{ GeV}$  when  $E_{\text{c.m.}} = 30 \text{ GeV}$ . We see from fig. 4 that although it would be less satisfying than a direct search for the  $\tilde{e}$ , one can probe higher values of  $m_{\tilde{e}}$  indirectly in a search for  $e^+e^- \rightarrow \gamma + \text{unobserved neutrals}$ . This domain of  $m_{\tilde{e}}$  is potentially interesting, since one class<sup>3</sup> of spontaneously broken supersymmetric models strongly suggests  $m_{\tilde{e}_{L,R}} \lesssim m_W/2$ , while another<sup>4,5</sup> might well have a comparably light  $\tilde{e}_R$ .

Going back now to fig. 2, the dashed vertical line corresponds to the maximum  $m_{\tilde{\gamma}}$  for which the cross section for  $e^+e^- \rightarrow \tilde{\gamma}\tilde{\gamma}\tilde{\gamma}$  is larger than  $10^{-38} \text{ cm}^2$  if  $m_{\tilde{e}} = 50 \text{ GeV}$ . This limit is of course independent of  $\sqrt{s}$  and comfortably includes the domain accessible to electron beam dump experiments.<sup>11</sup> A rough comparison suggests that while the effective  $e^+e^-$  annihilation luminosity in a beam dump is about five or six orders of magnitude larger than in high energy  $e^+e^-$  collisions, the  $s = E_{\text{c.m.}}^2$  value is about the same factor smaller. Therefore the  $s$ -dependence in the cross section formula [eq. (11)] compensates for the reduced luminosity and both classes of experiment are sensitive to similar ranges of  $m_{\tilde{e}}$ , though high energy  $e^+e^-$  collisions are sensitive to larger values of  $m_{\tilde{\gamma}}$  and all values of  $\sqrt{s}$ .

One might wonder whether one would be better off looking for photinos at higher energy  $e^+e^-$  machines. Clearly one would be sensitive to larger ranges of  $m_{\tilde{\gamma}}$ , but if  $m_{\tilde{\gamma}} \lesssim \text{few GeV}$ , one does not actually benefit from higher centre-of-mass energy, i.e., one does not gain access to much higher values of  $m_{\tilde{e}}$ . The reason is that while the cross section for  $e^+e^- \rightarrow \tilde{\gamma}\tilde{\gamma}\tilde{\gamma}$  rises

$\propto s = E_{\text{c.m.}}^2$  when  $E_{\text{c.m.}} \ll m_{\tilde{e}}$ , it turns over and starts falling when  $E_{\text{c.m.}} \gtrsim m_{\tilde{e}}$ . Moreover, there is a background from<sup>12</sup>  $e^+e^- \rightarrow \nu\bar{\nu}\gamma$  which is about  $2 \times 10^{-38} \times (s/900 \text{ GeV}^2)$  for  $E_{\text{c.m.}} \ll m_{Z^0}$ . The low-energy cross sections for  $e^+e^- \rightarrow \nu\bar{\nu}\gamma$  and  $\tilde{\gamma}\tilde{\gamma}\gamma$  are comparable if  $m_{\tilde{e}} \approx 50 \text{ GeV}$ , but at  $E_{\text{c.m.}} \gtrsim 30 \text{ GeV}$  the  $\nu\bar{\nu}\gamma$  cross section rises more rapidly than the  $\tilde{\gamma}\tilde{\gamma}\gamma$  cross section if  $m_{\tilde{e}} \lesssim 0(m_W)$ . Hence the signal-to-background ratio decreases at higher energies although the increase in the total number of events, which is roughly proportional to  $s = E_{\text{c.m.}}^2$ , does provide a statistical advantage  $\propto E_{\text{c.m.}}$  and thus enables one to measure the cross section for  $e^+e^- \rightarrow \gamma + \text{unobserved neutrals}$  more precisely. We have combined this statistical effect with the falling signal-to-background ratio in order to determine the maximum value of  $m_{\tilde{e}}$  that can be probed at different values of  $E_{\text{c.m.}}$ , assuming an integrated luminosity of  $100 \text{ pb}^{-1}$  as suggested at  $E_{\text{c.m.}} = 30 \text{ GeV}$ . The results for the case  $m_{\tilde{\gamma}} = 0$  are shown in fig. 5. We see that the sensitivity increases marginally from  $m_{\tilde{e}} = 59 \text{ GeV}$  at  $E_{\text{c.m.}} = 30 \text{ GeV}$  shown in fig. 4 to about  $60 \text{ GeV}$  when  $E_{\text{c.m.}} \approx 40 \text{ GeV}$ , and subsequently decreases when  $E_{\text{c.m.}} > 40 \text{ GeV}$ . We see that from this point of view the only advantage of higher  $E_{\text{c.m.}}$   $e^+e^-$  machines is the accessibility of higher gaugino masses.

We conclude this paper in the hope that we can convince our experimental colleagues that it is worthwhile to search for gauginos in present-day  $e^+e^-$  machines, both in the channel  $e^+e^- \rightarrow \gamma\gamma + \text{unobserved neutrals}$  and especially the channel  $e^+e^- \rightarrow \gamma + \text{unobserved neutrals}$ . Such searches have access to hitherto unexplored ranges of selectron and gaugino masses.

Acknowledgements

We thank our theoretical colleagues J. D. Bjorken, S. J. Brodsky, H. E. Haber and H. R. Quinn for informative discussions, and our experimental colleagues J. Dorfman, J.-P. Revol, R. Hollebeek and B. Richter for valuable advice and encouragement.

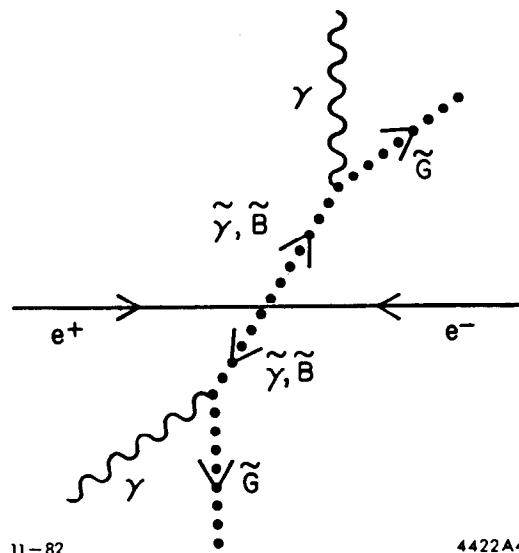
References

1. P. Fayet and S. Ferrara, Phys. Rep. 32C (1977) 249.
2. S. Dimopoulos and H. Georgi, Nucl. Phys. B193 (1981) 150;  
N. Sakai, Zeit. für Phys. C11 (1982) 153.
3. P. Fayet in "Unification of the Fundamental Particle Interactions,"  
eds. S. Ferrara, J. Ellis and P. Van Nieuwenhuizen (Plenum Press,  
N. Y., 1980), p. 587.
4. L. E. Ibáñez and G. G. Ross, Phys. Lett. 110B (1982) 215;  
J. Ellis, L. E. Ibáñez and G. G. Ross, Phys. Lett. 113B (1982) 283  
and CERN preprint TH-3383 (1982).
5. J. Ellis, J. S. Hagelin and D. V. Nanopoulos, Phys. Lett. 116B  
(1982) 283.
6. P. Fayet, École Normale Supérieure preprint LPTENS-82/12 (1982).
7. CELLO Collaboration, M. Davier, private communication (1982).
8. CELLO Collaboration, H. J. Behrend et al., Phys. Lett. 114B  
(1982) 287; TASSO Collaboration, R. Brandelik et al., DESY preprint  
82-032 (1982); JADE Collaboration, S. Komamiya, private communication  
(1982).
9. M. K. Gaillard, L. Hall and I. Hinchliffe, Phys. Lett. 116B (1982) 279.
10. J. Ellis and D. V. Nanopoulos, Phys. Lett. 110B (1982) 44;  
R. Barbieri and R. Gatto, Phys. Lett. 110B (1982) 211.
11. E-137 Collaboration, A. Abashian et al., request to SLAC EPAC for  
extension (1982).
12. E. Ma and J. Okada, Phys. Rev. Lett. 41 (1978) 287 and Phys. Rev. D18  
(1978) 4219; K. J. F. Gaemers, R. Gastmans and F. M. Renard, Phys.  
Rev. D19 (1979) 1605.

13. G. Barbiellini, B. Richter and J. L. Siegrist, Phys. Lett. 106B (1981) 414.
14. D. R. Yennie, S. Frautschi and H. Suura, Ann. Phys. 13 (1961) 379.
15. P. Salati and J. C. Wallet, LAPP preprint TH-65 (1982).

Figure Captions

- Fig. 1. Sketch of the possible signature for  $e^+e^- \rightarrow \tilde{\gamma}\tilde{\gamma}$  ( $\tilde{B}\tilde{B}$ ) followed by decays into  $\gamma + \tilde{G}$ . The photons have  $\langle E_\gamma \rangle = 1/4 E_{c.m.}$  each, do not come out back-to-back, and may not come from the annihilation vertex.
- Fig. 2. Regions of the  $m_{\tilde{\gamma}}, \sqrt{s}$  plane that are accessible to searches for  $e^+e^- \rightarrow \tilde{\gamma}\tilde{\gamma}$  (solid line) and  $e^+e^- \rightarrow \tilde{\gamma}\tilde{\gamma}\gamma$  (dashed line) with a sensitivity of  $10^{-38} \text{ cm}^2$  at  $E_{c.m.} = 30 \text{ GeV}$ .
- Fig. 3. Shape of the cross section for  $e^+e^- \rightarrow \gamma + \text{unobserved neutrals}$  (e.g.,  $\nu\bar{\nu}, \tilde{\gamma}\tilde{\gamma}$ ) as a function of  $\cos\theta_\gamma$  for lower limits on the photon energy  $x_\gamma \gtrsim 0.1, 0.2$ .
- Fig. 4. Domains of  $m_{\tilde{e}}$  and  $m_{\tilde{\gamma}}$  that are accessible to different searches in  $e^+e^-$  collisions at the level of  $10^{-38} \text{ cm}^2$ . The solid line derives from  $e^+e^- \rightarrow \tilde{\gamma}\tilde{\gamma}\gamma$ , the dashed line<sup>9,15</sup> from  $e^+e^- \rightarrow e\tilde{e}\tilde{\gamma}$  and the dotted line from  $\tilde{e}^+\tilde{e}^-$  pair production.<sup>8</sup>
- Fig. 5. Sensitivity to  $m_{\tilde{e}}$  via the reaction  $e^+e^- \rightarrow \tilde{\gamma}\tilde{\gamma}\gamma$  as a function of the centre-of-mass energy.



11-82

4422A4

Fig. 1



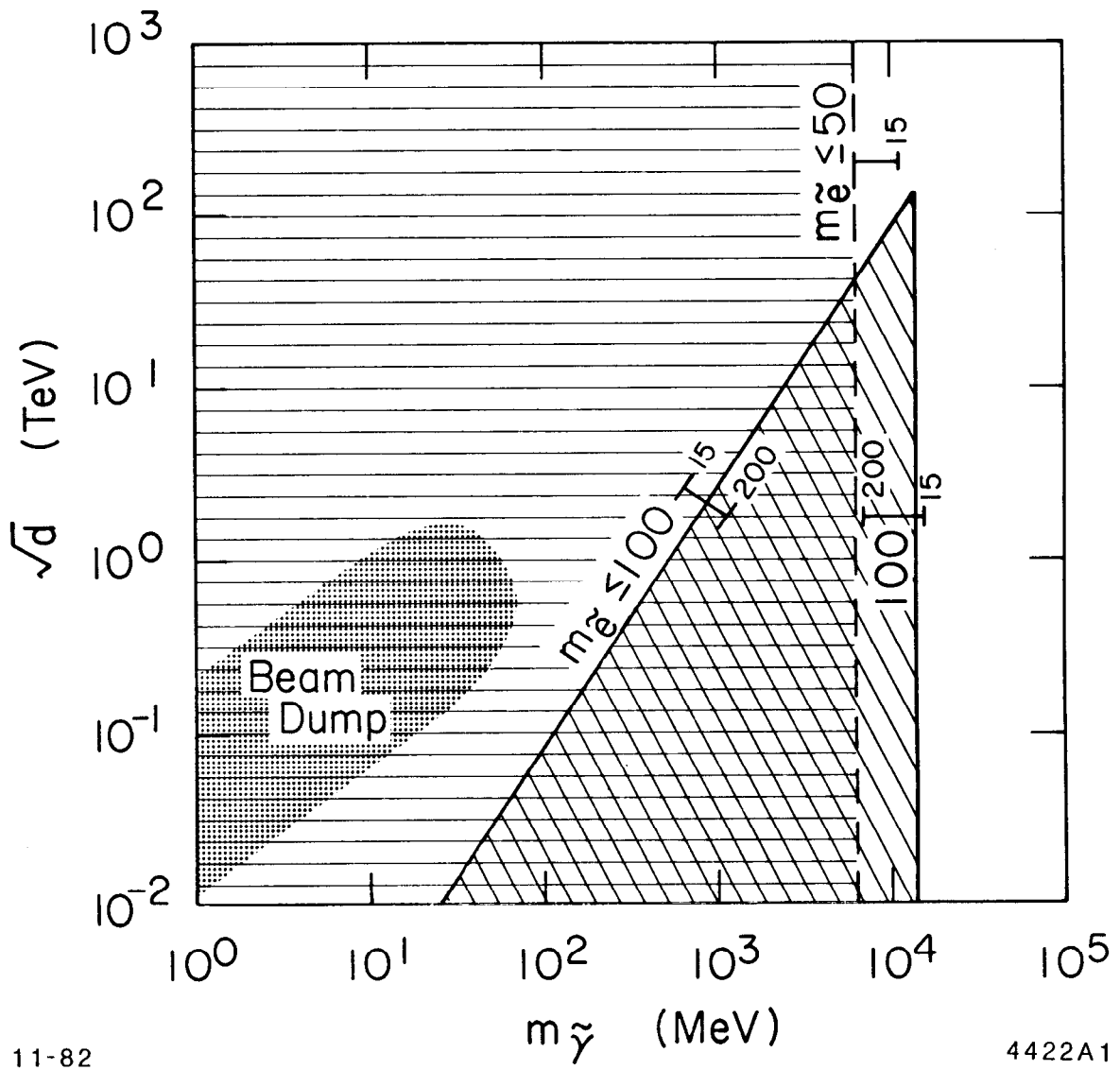


Fig. 2

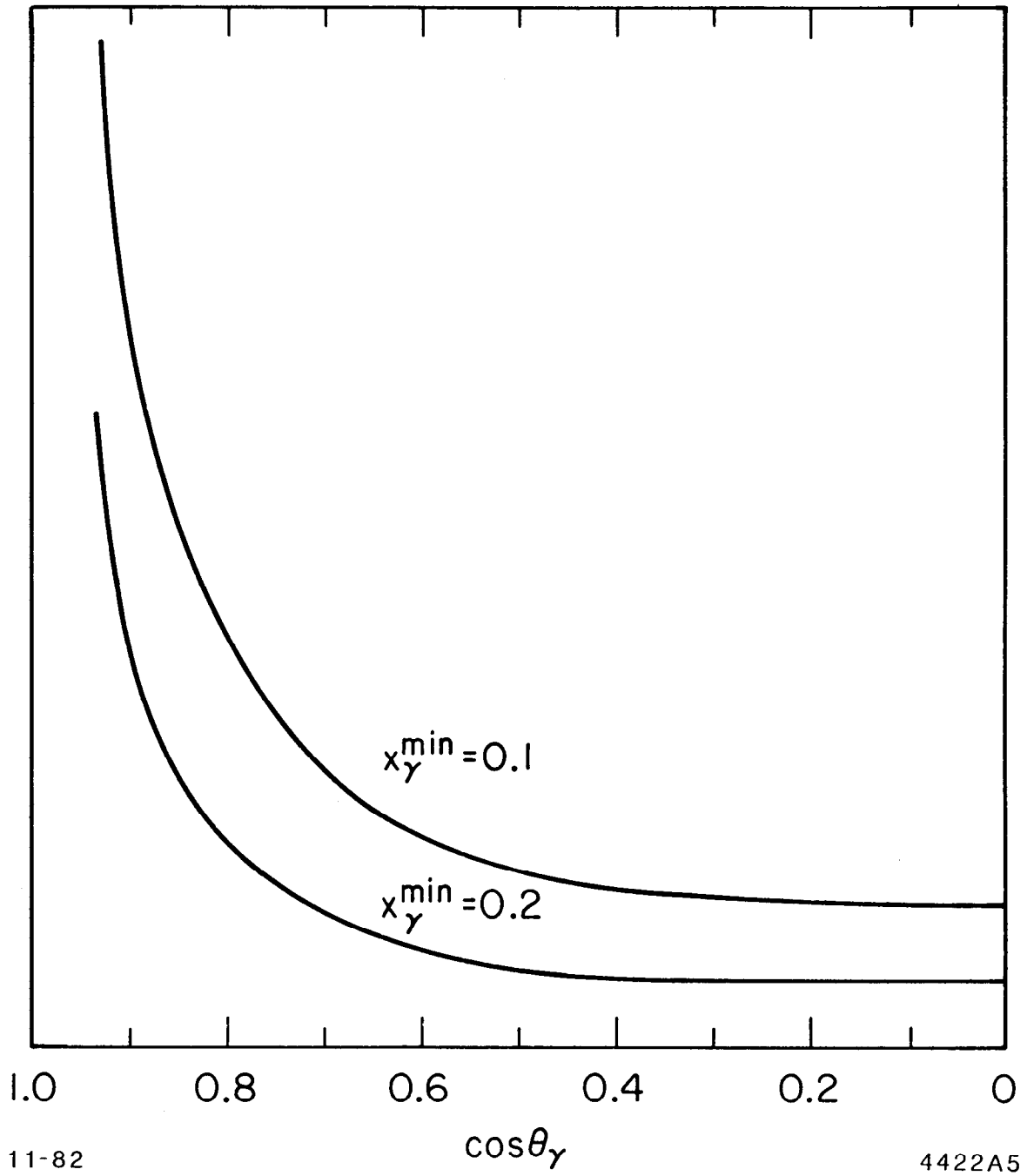


Fig. 3

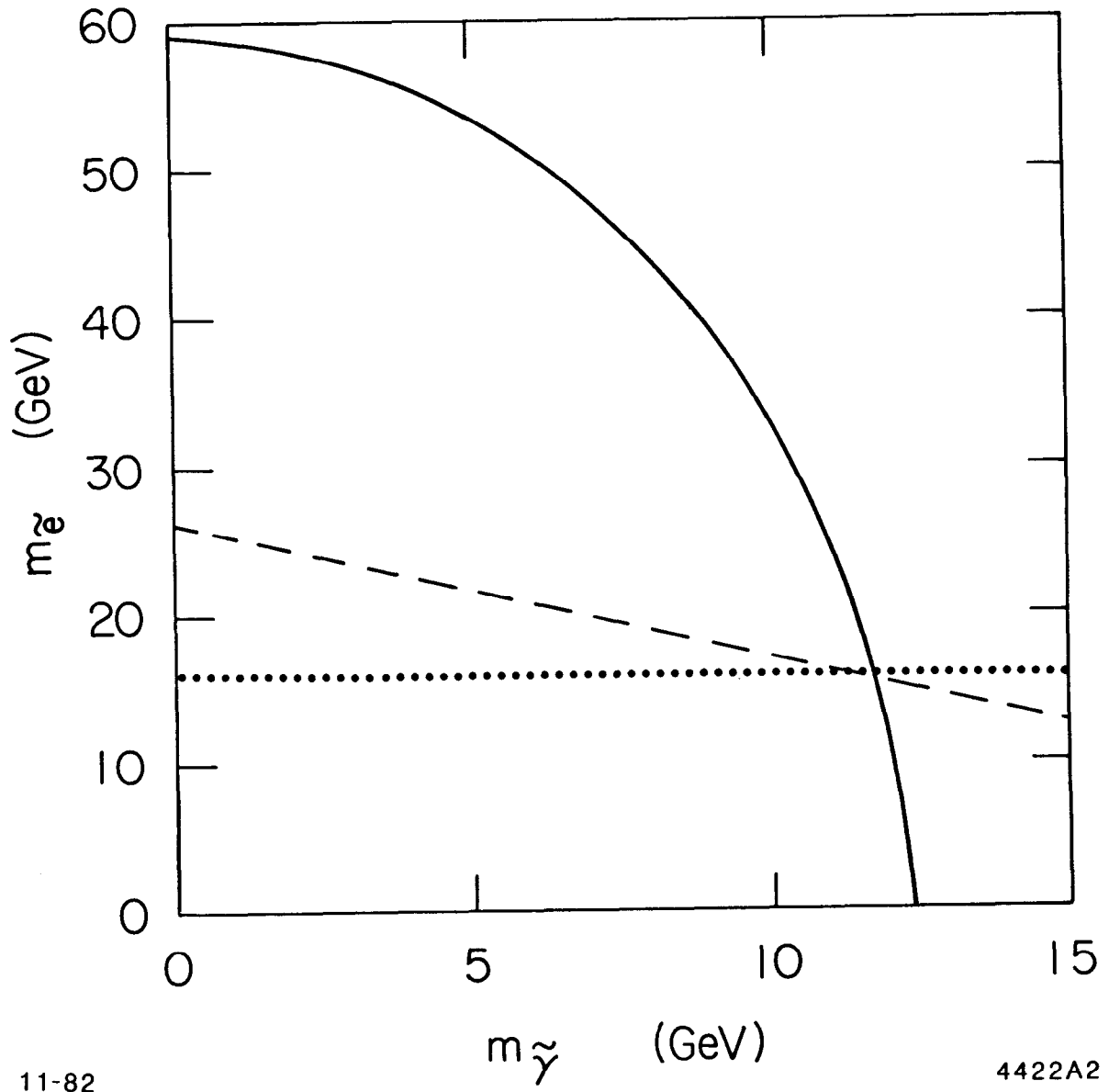


Fig. 4

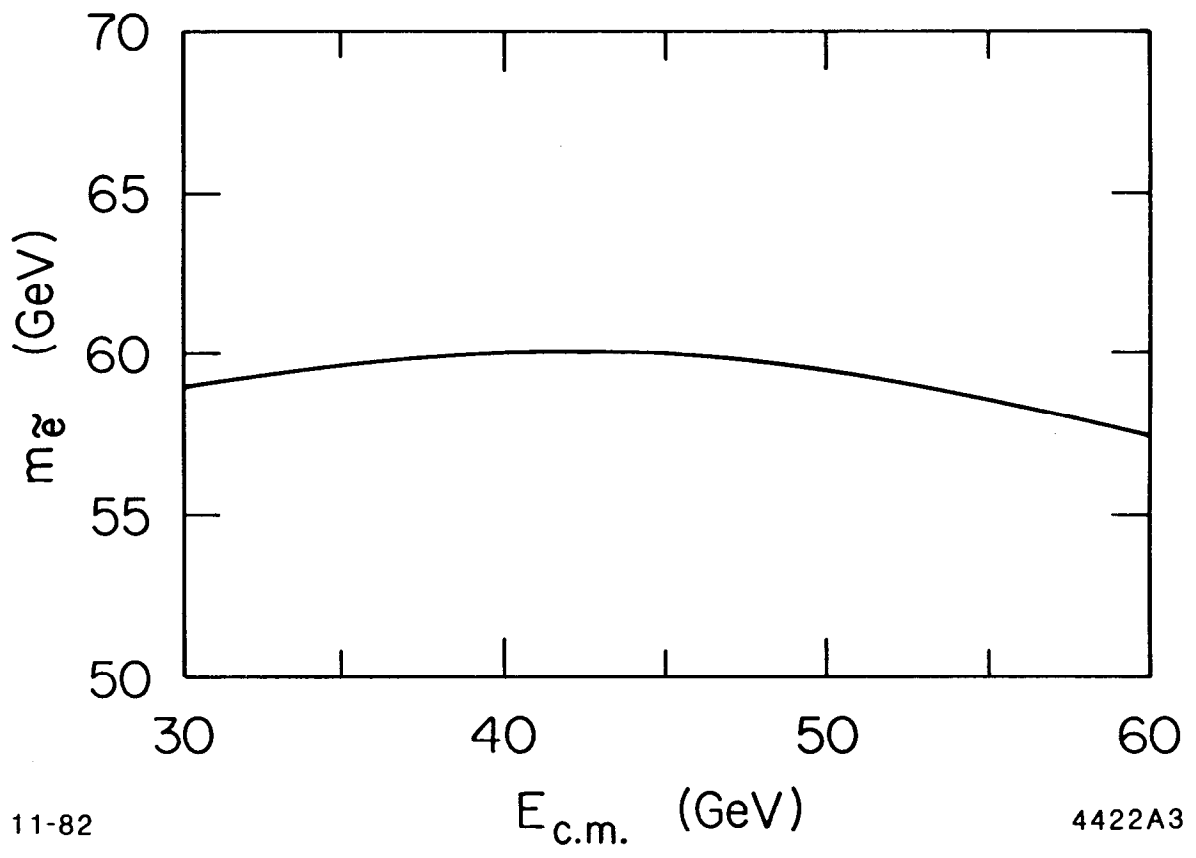


Fig. 5